DOI: 10.1002/ejic.200701358

Syntheses, Characterization, and Reactivities of (μ-η^2:η^2-Disulfido)dicopper(II) Complexes with *N*-Alkylated *cis*,*cis*-1,3,5-Triaminocyclohexane Derivatives

Yuji Kajita,[a] Jun Matsumoto,[a] Isao Takahashi,[b] Shun Hirota,[b,c] Yasuhiro Funahashi,[a] Tomohiro Ozawa,[a] and Hideki Masuda*[a]

Keywords: Disulfide / Dicopper complexes / Triaminocyclohexane / Dihedral angles

Three novel (disulfido)dicopper(II) complexes with *N*-alkylated *cis,cis*-1,3,5-triaminocyclohexane derivatives, $[Cu_2(S_2)(R_3TACH)]X_2$ [(R, X) = (Et, CF_3SO_3) (**1**), (*i*Bu, SbF_6) (**2**), and (Bn, SbF_6) (**3**)], have been synthesized and characterized by elemental, electrochemical, and X-ray structure analyses, and electronic absorption, IR, ESI mass, and resonance Raman spectroscopic methods. The X-ray crystal structures indicate that the two sulfur and two copper atoms of these complexes form a $Cu_2(S_2)$ structure with slight bending of the two planes defined by the CuS_2 plane at angles of 166.12° (the individual bending angles are 175.56° for **1a** and 156.67° for **1b**), 154.74°, and 180° for **1**, **2**, and **3**, respectively. The UV/Vis absorption spectra of **1**, **2**, and **3** have a sharp band at ca. 360 nm with a broadened shoulder at 400–480 nm and low intensity d–d bands in the range 666–671 nm. The resonance Raman spectra of the complexes have peaks assignable to a ν(S–S) band at 483–484 cm^{-1}. The complexes have reduction waves at –974 to –946 vs. $[Fe(C_5H_5)_2]/[Fe(C_5H_5)_2]^+$ for **1**, –993 to –976 for **2**, and –948 to –928 mV for **3**. These values are in a low-potential region relative to bis(μ-OH)dicopper complexes with R_3TACH. This may be explained by the occurrence of strong π-donation from the disulfide ligands as observed for previously reported (disulfido)Ru complexes. Compounds **1**, **2**, and **3** react with PPh_3 to give $S{=}PPh_3$ in yields of 65 ± 3.5, 76 ± 1, and 50 ± 2 %, respectively. These results are discussed in terms of the relationship between the dihedral angles in the $Cu_2(S_2)$ core and the reactivity of S_2^{2-}.

Introduction

Sulfur is an essential element found in amino acids and proteins that play important roles in the metabolism of all living organisms. Recently, the crystal structure of nitrous oxide reductase (N_2OR), a copper-containing enzyme, has been determined by X-ray analysis.[1–11] In this metalloprotein the two metal centers designated as Cu_A and Cu_Z have dinuclear and tetranuclear copper coordination structures, respectively. The Cu_A site functions as an electron-transfer site, while the Cu_Z site acts as a catalytic site. The Cu_Z site has a particularly interesting structure with a mixed-valence metal cluster $[Cu_4S]^{n+}$ that forms a distorted tetrahedron comprised of four copper atoms bridged by a sulfido ion (Figure 1). This structure represents the first example of a biological system that includes an inorganic sulfide ion as part of a multi-copper cluster.[4–6,8,11]

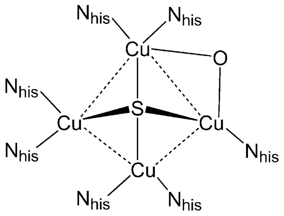

Figure 1. Structure of Cu_Z site of N_2OR.

Recently, some (disulfido)dicopper(II) complexes with bi-, tri-, and tetradentate ligands (Figure 2)[12–21] have been reported as structural analogues of (μ-peroxido)dicopper complexes.[22–28] However, the chemical properties of (disulfido)dicopper complexes are different from those of (μ-peroxido)dicopper complexes. It is thus interesting to compare (μ-disulfido)- and (μ-peroxido)dicopper(II) complexes.[29,30] In these studies, methods for synthesizing the (disulfido)dicopper complexes as well as crystal structures and reactivities of the complexes with exogenous substrates are discussed. The chemical features of (disulfido)dicopper complexes, however, have not yet been clarified in detail. We report herein on the syntheses and characterization of three novel (disulfido)dicopper(II) complexes with *N*-alkylated *cis,cis*-1,3,5-triaminocyclohexane derivatives (R_3TACH) (R = Et, *i*Bu, and Bn)[31,32] with the aim of gaining an improved understanding of the chemical features of (di-

---

[a] Department of Applied Chemistry, Faculty of Engineering, Nagoya Institute of Technology,
Showa-ku, Nagoya 466-8555, Japan
Fax: +81-52-735-5209
E-mail: masuda.hideki@nitech.ac.jp
[b] Graduate School of Materials Science, Nara Institute of Science and Technology,
8916-5 Takayama, Ikoma, Nara 630-0192, Japan
[c] PRESTO, JST,
Kawaguchi, Saitama 322-0012, Japan

Supporting information for this article is available on the WWW under http://www.eurjic.org or from the author.

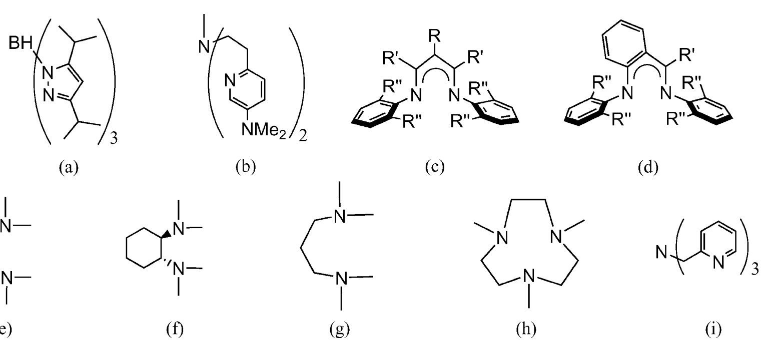

Figure 2. Examples of bi-, tri-, and tetradentate supporting ligands.

sulfido)dicopper complexes. R_3TACH ligands have a high affinity for copper, stabilize the coordination structure with three rigid six-membered chelate rings constrained by the cyclohexane framework, provide strong σ-donation to copper ions, and provide a means for introducing various *N*-alkyl substituents. Furthermore, we have also investigated their reactivity with exogenous substrates. From these results the relationships between structural features and reactivities are discussed.

Results and Discussion

Synthesis of (Disulfido)dicopper(II) Complexes

The series of (μ-η^2:η^2-disulfido)dicopper(II) complexes with *cis,cis*-1,3,5-triaminocyclohexane derivatives R_3TACH (R = Et, *i*Bu, and Bn), **1**, **2**, and **3**, respectively, are isolated as reddish brown crystals from reaction solutions of the Cu^I complexes [Cu(MeCN)(R_3TACH)]X (R = Et, *i*Bu, and Bn, X = SbF_6 or CF_3SO_3) with S_8 in CH_2Cl_2, toluene, or Et_2O at room temperature under Ar. The products were characterized by IR, UV/Vis, ESI-TOF/mass, and resonance Raman spectroscopy as well as by elemental (C, H, and N) and X-ray crystallographic analyses. The disulfido complexes **1**, **2**, and **3** are air-stable at room temperature in the solid state. In solution, the colors of these complexes change from brown to green, and precipitate as black solids in air. This most likely indicates that **1**, **2**, and **3** react with dioxygen or water in solution to form CuS.

The ^{1}H NMR spectra of **1**, **2**, and **3** in [D_6]DMSO at room temperature have peaks in the diamagnetic region of δ = 1–10 ppm. These complexes are ESR-silent in CH_2Cl_2 at 77 K. These results indicate the occurrence of strong antiferromagnetic coupling between two Cu^{II} ions in the $Cu_2(S_2)$ core.

Crystal Structures of (Disulfido)dicopper(II) Complexes

The crystal structures of (disulfido)dicopper(II) complexes, **1**, **2**, and **3**, were determined by X-ray structural analyses. The ORTEP views of **1a** and **1b** are shown in Figure 3 and those of **2** and **3** in Figure 4, and selected bond lengths and angles are listed in Table 1 for **1** (**1a** and **1b**) and Table 2 for **2** and **3**. The coordination geometries of each of the complexes **1**, **2**, and **3** are square-pyramidal with the two S atoms and two N atoms of the TACH ligand in the equatorial plane and one N atom of the TACH ligand at the axial site.

The crystal structure of **1** contains two crystallographically independent molecules, **1a** and **1b**, in the unit cell. For **1a**, the amine nitrogen atoms (N3/N4) and the methylene moiety (C11/C12) of one ethyl group of Et_3TACH are disordered. In the structure of **1b** the methylene (C32/C33/C34) and methyl carbon atoms (C35/C36) of one ethyl

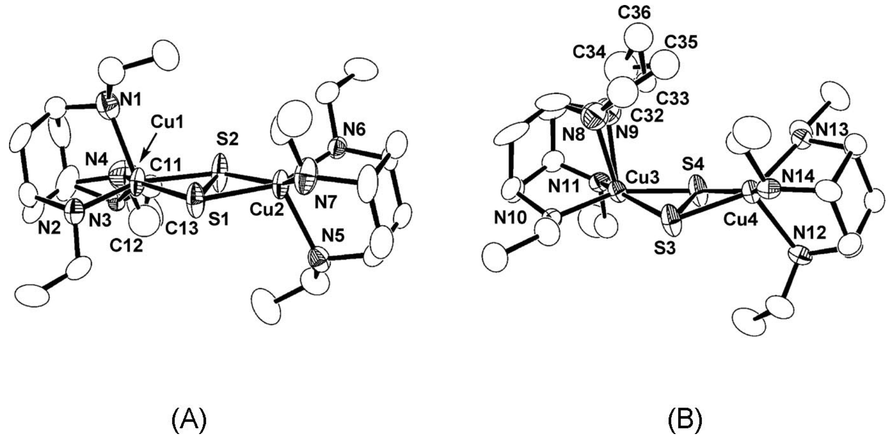

Figure 3. ORTEP views (50% probability) of cation parts of **1a** (A) and **1b** (B). Hydrogen atoms are omitted for clarity.

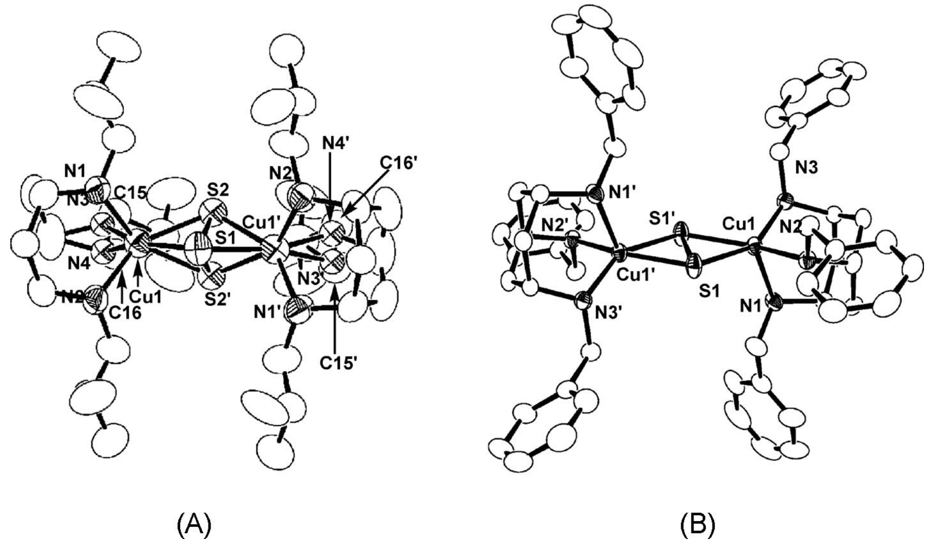

Figure 4. ORTEP views (50% probability) of cation parts of **2** (A) and **3** (B). Hydrogen atoms are omitted for clarity.

Table 1. Selected bond lengths [Å] and angles [°] for **1a** and **1b**.

1a				**1b**			
Cu1–S1	2.253(2)	Cu1–S2	2.2426(19)	Cu3–S3	2.2362(19)	Cu3–S4	2.245(2)
Cu1–N1	2.189(5)	Cu1–N2	2.011(6)	Cu3–N8	2.240(13)	Cu3–N9	2.192(13)
Cu1–N3	2.057(10)	Cu1–N4	2.06(2)	Cu3–N10	2.017(5)	Cu3–N11	2.011(4)
Cu2–S1	2.253(2)	Cu2–S2	2.228(2)	Cu4–S3	2.241(2)	Cu4–S4	2.2457(18)
Cu2–N5	2.184(4)	Cu2–N6	2.023(5)	Cu4–N12	2.168(5)	Cu4–N13	2.027(5)
Cu2–N7	2.043(7)	S1–S2	2.101(3)	Cu4–N14	2.010(4)	S3–S4	2.116(2)
Cu1···Cu2	3.9629(10)			Cu3···Cu4	3.8710(12)		
S1–Cu1–S2	55.72(9)	S1–Cu1–N1	116.86(18)	S3–Cu3–S4	56.37(7)	S3–Cu3–N8	104.1(3)
S1–Cu1–N2	98.02(18)	S1–Cu1–N3	142.1(2)	S3–Cu3–N9	110.7(4)	S3–Cu3–N10	102.05(15)
S1–Cu1–N4	148.0(4)	S2–Cu1–N1	104.59(18)	S3–Cu3–N11	150.71(17)	S4–Cu3–N8	107.8(4)
S2–Cu1–N2	152.49(17)	S2–Cu1–N3	102.9(2)	S4–Cu3–N9	97.5(4)	S4–Cu3–N10	155.12(15)
S2–Cu1–N4	94.8(5)	N1–Cu1–N2	94.4(2)	S4–Cu3–N11	98.84(18)	N8–Cu3–N9	17.4(5)
N1–Cu1–N3	97.8(2)	N1–Cu1–N4	79.8(4)	N8–Cu3–N10	88.4(4)	N8–Cu3–N11	98.1(3)
N2–Cu1–N3	93.8(3)	N2–Cu1–N4	108.2(5)	N9–Cu3–N10	102.3(5)	N9–Cu3–N11	86.0(3)
N3–Cu1–N4	22.3(4)	S1–Cu2–S2	55.92(9)	N10–Cu3–N11	97.4(2)	S3–Cu4–S4	56.29(7)
S1–Cu2–N5	107.28(15)	S1–Cu2–N6	152.90(14)	S3–Cu4–N12	108.38(15)	S3–Cu4–N13	151.34(15)
S1–Cu2–N7	97.18(19)	S2–Cu2–N5	114.26(16)	S3–Cu4–N14	98.26(18)	S4–Cu4–N12	104.09(13)
S2–Cu2–N6	99.63(16)	S2–Cu2–N7	146.49(17)	S4–Cu4–N13	102.45(14)	S4–Cu4–N14	151.41(18)
N5–Cu2–N6	92.9(2)	N5–Cu2–N7	91.3(2)	N12–Cu4–N13	94.7(2)	N12–Cu4–N14	95.97(19)
N6–Cu2–N7	100.3(2)			N13–Cu4–N14	95.86(19)		

group of Et_3TACH are also disordered. The dihedral angles between the two CuS_2 planes are 175.56° and 156.67° for **1a** and **1b**, respectively, and the dihedral angle for **1b** is more bent than that of **1a**. The Cu···Cu/S–S distances are 3.9629(10)/2.101(3) Å for **1a** and 3.8710(12)/2.116(2) Å for **1b**. The two ethyl substituents of the equatorial amine nitrogen atoms are spread out from the Cu^{II} ion, while the remaining ethyl substituent at the axial nitrogen atom points toward the Cu^{II} ion in both **1a** and **1b**. In the crystal structure of **2**, the amine nitrogen (N3/N4) and μ-sulfido (S2/S2′) atoms are disordered. The Cu···Cu/S–S distances are 3.8445(18)/2.093(6) Å. All isobutyl groups in this structure spread out from the Cu^{II} ion. One sulfur atom (S2) of the bridging μ-disulfido ligand is highly disordered. The dihedral angle between the two CuS_2 planes of **2** is 154.74°. In the crystal structure of **3**, the Cu···Cu/S–S distances are 3.9197(7)/2.1213(18) Å, and the dihedral angle between the CuS_2 planes is 180°. The Cu···Cu distance [3.8445(18)] of **2** is the shortest among the (disulfido)dicopper complexes with R_3TACH, which originates from the most bent dihedral angle in **2** (154.74°). This relationship between metal–metal distances and dihedral angles has also been reported previously for many bis(μ-OH)dicopper(II) complexes.[33–44] The τ values of the complexes (defined as 0 for an idealized square pyramid and 1 for an idealized trigonal bipyramid) were found to be 0.07–0.16/0.11 for **1a**, 0/0.07 for **1b**, 0.21–0.17 for **2**, and 0.04 for **3**.[45] This shows that the coordination geometries of **1a**, **1b**, **2**, and **3** are distorted square-pyramidal structures.

Tolman and co-workers have reported on the relationship between the Cu···Cu, Cu–S, and S–S distances and the degree of S–S bond activation in many (disulfido)dicopper

Table 2. Selected bond lengths [Å] and angles [°] for **2** and **3**.

2				**3**			
Cu1–S1	2.174(2)	Cu1–S2	2.292(5)	Cu1–S1	2.2339(13)	Cu1–S1′	2.2229(13)
Cu1–S2′	2.295(5)	Cu1–N1	2.080(9)	Cu1–N1	2.195(3)	Cu1–N2	2.002(3)
Cu1–N2	2.091(8)	Cu1–N3	2.039(16)	Cu1–N3	2.024(3)	S1–S1′	2.1213(18)
Cu1–N4	2.037(17)	S1–S2	2.093(6)	Cu1···Cu1′	3.9197(7)		
S1–S2′	2.093(6)	S2–S2′	1.777(8)				
Cu1···Cu1′	3.8445(18)						
S1–Cu1–S2	55.82(16)	S1–Cu1–S2′	55.77(16)	S1–Cu1–S1′	56.84(4)	S1–Cu1–N1	112.98(10)
S1–Cu1–N1	96.7(2)	S1–Cu1–N2	95.8(2)	S1–Cu1–N2	96.95(10)	S1–Cu1–N3	150.55(10)
S1–Cu1–N3	159.5(4)	S1–Cu1–N4	158.2(4)	S1′–Cu1–N1	103.10(10)	S1′–Cu1–N2	152.80(10)
S2–Cu1–S2′	45.6(2)	S2–Cu1–N1	107.2(2)	S1′–Cu1–N3	100.56(10)	N1–Cu1–N2	93.57(13)
S2–Cu1–N2	147.1(2)	S2–Cu1–N3	103.8(4)	N1–Cu1–N3	89.04(13)	N2–Cu1–N3	101.07(14)
S2–Cu1–N4	111.5(5)	S2′–Cu1–N1	147.9(2)				
S2′–Cu1–N2	106.6(2)	S2′–Cu1–N3	112.7(4)				
S2′–Cu1–N4	102.5(5)	N1–Cu1–N2	91.0(3)				
N1–Cu1–N3	87.7(5)	N1–Cu1–N4	104.5(5)				
N2–Cu1–N3	104.1(5)	N2–Cu1–N4	89.1(5)				
N3–Cu1–N4	22.2(6)						

complexes.[11,18] In these reports it was indicated that high S–S bond activation appears in complexes with short Cu···Cu and Cu–S bonds and with long S–S bonds. The S–S bonds of **1**, **2**, and **3** are longer than that of $[Cu_2(S_2)(Tp^{iPr2})_2]$ [Tp^{iPr2} = hydridotris(3,5-diisopropyl-1-pyrazolyl)borate] [2.073(4) Å], and are shorter than those of (μ-η^2:η^2-disulfido)dicopper complexes with diketiminate, anilido–imine derivatives, or Me_3tacn [2.165(4)–2.2140(10) Å] (Me_3tacn = 1,4,7-trimethyl-1,4,7-triazacyclononane). The S–S bond lengths are close to those of $[Cu_2(S_2)(Me_2NPY2)_2][B(C_6F_5)_4]_2$ [Me_2NPY2 = bis({2-[4-(dimethylamino)pyridyl]ethyl}methyl)amine] [2.117(2) Å] and $[Cu_2(S_2)(Me_4pda)_2(CF_3SO_3)_2]$ (Me_4pda = *N*,*N*,*N*′,*N*′-tetramethylpropanediamine) [2.105(4) Å].[12,17,18,21] Thus, in (μ-η^2:η^2-disulfido)dicopper complexes with R_3TACH, the S–S bond activations were expected to be lower than those of (μ-η^2:η^2-disulfido)dicopper complexes with diketiminate, anilido–imine derivatives, or Me_3tacn. The Cu–S distances of **1**, **2**, and **3** are particularly longer than that of $[Cu_2(S_2)(Me_3tacn)_2][SbF_6]_2$, although **1**, **2**, and **3** have an alkylamine tridentate ligand similar to Me_3tacn. This may indicate that $Cu^{II}d_{xy} \rightarrow S_2^{2-}\sigma^*$ back-bonding is weakened due to the small dihedral angles between the two CuS_2 planes. In fact, there is a trend toward elongation of the Cu–S distances as the dihedral angles decrease between two CuS_2 planes in **1**, **2**, and **3**. It remains difficult to rationalize the observation that the $Cu_2(S_2)$ core in **1b** and **2** is bent.

UV/Vis Spectra of 1, 2, and 3

UV/Vis spectra of **1**, **2**, and **3** are shown in Figure 5, and their spectroscopic data are provided in Table 3. All of the spectra exhibit an intense band with two broadened shoulders and one additional smaller band: 359 (ε = 21100 $cm^{-1}\,M^{-1}$), 408 (sh, 9800), 470 (sh, 6700), and 669 (sh, 750) nm for **1**, 363 (20400), 413 (sh, 11300), 478 (sh, 7800), and 671 (sh, 450) nm for **2**, and 361 (17200), 402 (11000), 458 (sh, 7000), and 666 (sh, 380) nm for **3**. The bands at 359–363 nm and 458–478 nm were assigned to the in-plane disulfido-π^*_σ-to-Cu^{II} charge-transfer (CT) transition, and the shoulders at 402–413 nm were assigned to the out-of-plane disulfido-π^*_v-to-Cu^{II} CT on the basis of the previously reported data of (μ-η^2:η^2-disulfido)dicopper complexes.[12,14,17,18,29] The weak bands at 666–671 nm were assigned to d–d transitions. In the UV/Vis absorption spectra, **1**, **2**, and **3** exhibit similar spectra indicating that the structures of **1**, **2**, and **3** are similar in solution. The UV/Vis reflectance spectra of **1**, **2**, and **3** have peaks at 263, 348, 388, and 716 nm for **1**, 256, 360, 413, 480, and 570 nm for **2**, and 298, 356, 402, 450, and 664 nm for **3**. These results indicate that the coordination geometries of the Cu^{II} ions

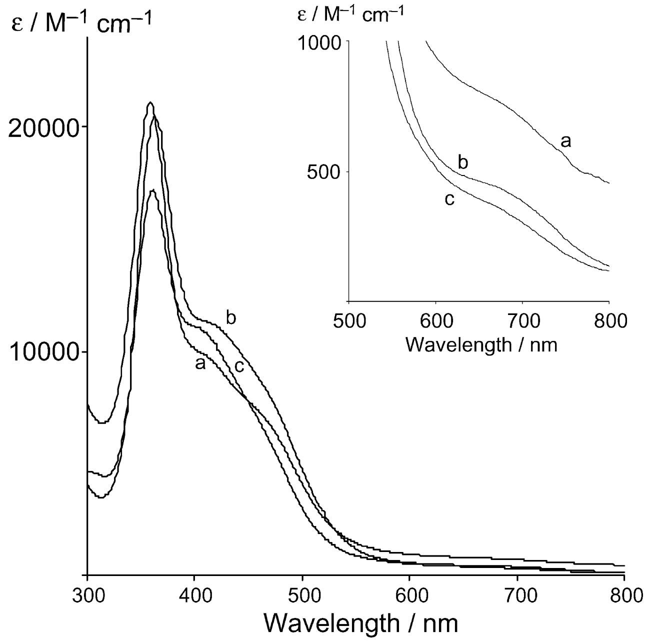

Figure 5. UV/Vis absorption spectra of **1** (spectrum a), **2** (spectrum b), and **3** (spectrum c). Inset: expanded view in the 500–800 nm region.

Table 3. UV/Vis and resonance Raman spectral data for side-on (disulfido)dicopper(II) complexes.

Compound	λ_{max} [nm] (ε [$\mathrm{M^{-1}\,cm^{-1}}$])	ν(S–S) [$\mathrm{cm^{-1}}$] ($\Delta\nu$ [$\mathrm{cm^{-1}}$])	Ref.
1	359 (21100), 408 (sh. 9800), 470 (sh. 6700), 669 (750)	483 (13)	this work
2	363 (20400), 413 (sh. 11300), 478 (sh. 7800), 671 (450)	484 (12)	this work
3	361 (17200), 402 (sh. 11000), 458 (sh. 7000), 666 (380)	483 (13)	this work
$[Cu_2(S_2)(Tp^{3,5\text{-}i\mathrm{Pr}})_2]$	355 (31200), 479 (3500), 660 (190)	500 (12)	[12,29]
$[Cu_2(S_2)(Me_2NPY2)_2](B(C_6F_5)_4)_2)$	315 (13900), 395 (3700), 460 (1850), 630 (460)		[17]
$[Cu_2(S_2)(Me_3tacn)_2](SbF_6)_2$	269 (5800), 397 (14300)	477 (14)	[21]
$[Cu_2(S_2)(Me_4pda)_2](CF_3SO_3)_2$	254 (4800), 370 (11000)	485 (15)	[21]
$[Cu_2(S_2)\{H(Me_2L^{Me2})\}_2]$	352 (12000), 427 (8200), 540 (400), 804 (130)	442 (9)	[18]
$[Cu_2(S_2)\{H(Me_2L^{Et2})\}_2]$	432 (24200), 541 (900), 806 (300)	443 (10)	[14,18]
$[Cu_2(S_2)\{H(t\mathrm{Bu}_2L^{i\mathrm{Pr}2})\}_2]$		454 (13)	[18]
$[Cu_2(S_2)\{Ph(H_2L^{Et2})\}_2]$	387 (34376), 421 (23470), 588 (1260), 813 (310)	424 (10)	[18]
$[Cu_2(S_2)\{Ph(H_2L^{i\mathrm{Pr}2})\}_2]$	386 (32410), 432 (24350), 612 (1290)	435 (8)	[18]
$[Cu_2(S_2)\{3,5\text{-}(CF_3)_2C_6H_3(H_2L^{Me2})\}_2]$	377 (32900), 421 (25500), 547 (1400), 827 (600)	441 (9)	[18]
$[Cu_2(S_2)\{3,5\text{-}(CF_3)_2C_6H_3(H_2L^{i\mathrm{Pr}2})\}_2]$	381 (26200), 434 (22800), 575 (1300), 830 (290)	428 (12)	[18]
$[Cu_2(S_2)(HL'^{Me2})_2]$	435 (29100), 604 (1300), 815 (400)	432 (8)	[18]
$[Cu_2(S_2)(HL'^{i\mathrm{Pr}2})_2]$	448 (31600), 533 (1300), 865 (400)	440 (13)	[14,18]
$[Cu_2(S_2)(MeL'^{i\mathrm{Pr}2})_2]$	437 (17700), 460 (21600), 651 (1000), 877 (120)	443 (11)	[18]

of **1** and **3** in solution are the same as the solid-state geometries. However, the copper coordination geometries of **2** in solution may be more distorted from a square pyramid than in the solid-state geometry because the d–d band in solution is shifted 100 nm to a lower energy region relative to that in the solid state.[46]

Resonance Raman Spectra of 1, 2, and 3

The S–S stretching vibrations [ν(S–S)] for **1**, **2**, and **3** were obtained by resonance Raman measurements in CH_2Cl_2 at ambient temperature (excitation at 457.9 nm). The spectra of **1**, **2**, and **3** are shown in Figure 6, and the selected spectroscopic data are listed in Table 3. The $\nu(^{32}S\text{–}^{32}S)$ bands of **1**, **2**, and **3** are detected at 483, 484, and 483 $\mathrm{cm^{-1}}$, respectively, and the isotope shifts ($\Delta\nu$) of these bands are 13, 12, and 13 $\mathrm{cm^{-1}}$, respectively.[12,18,29,47] These three ν(S–S) values are essentially identical, although the molecular sizes of *N*-alkyl substituents for **1**, **2**, and **3** are different (ethyl, isobutyl, and benzyl). This result indicates that the *N*-alkyl substituent groups of the complexes do not affect the $Cu_2(S_2)$ core. The dihedral angles of the $Cu_2(S_2)$ core also do not influence the ν(S–S) values of **1**, **2**, and **3**. The locations of the ν(S–S) bands of **1**, **2**, and **3** are close to the positions of the analogous bands of $[Cu_2(S_2)(Me_4pda)_2\text{-}(CF_3SO_3)_2]$ (485 $\mathrm{cm^{-1}}$), although they were observed in a lower energy region than the analogous bands of $[Cu_2(S_2)(Tp^{i\mathrm{Pr}2})_2]$ (500 $\mathrm{cm^{-1}}$) and in a higher energy region than those of (μ-η^2:η^2-disulfido)dicopper complexes with diketiminate, anilido–imine derivatives, and Me_3tacn (424–454 and 477 $\mathrm{cm^{-1}}$).[12,18,21,29] Thus, the S–S bonds of (disulfido)dicopper complexes with R_3TACH are weaker than those of $[Cu_2(S_2)(Tp^{i\mathrm{Pr}2})_2]$ and are stronger than those of (μ-η^2:η^2-disulfido)dicopper complexes with diketiminate, anilido–imine derivatives, or Me_3tacn. These results agree well with the S–S bond lengths of the crystal structures.

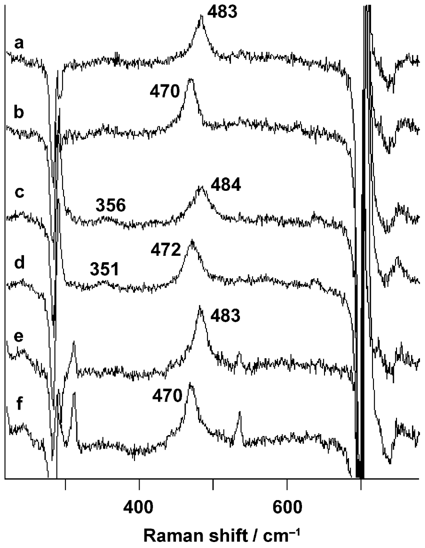

Figure 6. Resonance Raman spectra of **1** prepared by using $^{32}S_8$ (spectrum a), **1** prepared by using $^{34}S_8$ (spectrum b), **2** prepared by using $^{32}S_8$ (spectrum c), **2** prepared by using $^{34}S_8$ (spectrum d), **3** prepared by using $^{32}S_8$ (spectrum e), **3** prepared by using $^{34}S_8$ (spectrum f).

For complex **2**, the $\nu(Cu\text{–}^{32}S)$ band was observed at 356 $\mathrm{cm^{-1}}$ [$\nu(Cu\text{–}^{34}S)$ = 351 $\mathrm{cm^{-1}}$] as a very small peak. This small peak was assigned as a Cu–S stretching band, because the isotope effect of $\Delta\nu[(Cu\text{–}^{32}S) - (Cu\text{–}^{34}S)]$ (5 $\mathrm{cm^{-1}}$) was detected. This ν(Cu–S) value is much lower than that of the previously reported side-on (disulfido)dicopper complex $[Cu_2(S_2)(Tp^{i\mathrm{Pr}2})_2]$ (495 $\mathrm{cm^{-1}}$). The $\nu(\text{Cu–S})_{sym}$ bands of end-on (disulfido)dicopper complexes $[Cu_2(\mu\text{-}1,2\text{-}S_2)\text{-}(TMPA)_2]^{2+}$ and $[Cu_2(\mu\text{-}1,2\text{-}S_2)(TMPA')_2]^{2+}$ [TMPA = tris(2-pyridylmethyl)amine, TMPA′ = bis(2-pyridylmethyl)-(6-methoxymethyl-2-pyridylmethyl)amine] are observed at 316 and 309 $\mathrm{cm^{-1}}$, respectively, and the ν(Cu–S) frequency of **2** is similar to the ν(Cu–S) frequencies of end-on (disulfido)dicopper complexes.[13,29,48] Regrettably, we could not make a definitive assignment for the peak at 356 $\mathrm{cm^{-1}}$.

Electrochemical Properties

The redox potentials of **1**, **2**, and **3** in DMF and CH_2Cl_2 were determined by cyclic voltammetry measurements. The voltammograms of **1**, **2**, and **3** are shown in Figure 7, and their anodic and cathodic peaks are listed in Table 4. It has been reported that the reduction wave of a (μ-η^2:η^2-disulfido)dicopper(II) complex with the peralkylated triamine ligand, Me_3tacn, was observed at –750 mV vs. $[Fe(C_5H_5)_2]/[Fe(C_5H_5)_2]^+$.[21] The reduction waves of **1**, **2**, and **3** were observed in the range –993 to –928 mV {vs. $[Fe(C_5H_5)_2]/[Fe(C_5H_5)_2]^+$}, which were assigned to $Cu^{I/II}$ reduction peaks of (disulfido)dicopper complexes **1**, **2**, and **3**, because these reduction waves in both solvents are observed in the same region and because they are similar to the redox potentials of the previously reported bis(μ-hydroxido)dicopper(II) complexes with R_3TACH $[Cu_2(OH)_2(R_3TACH)_2]^{2+}$ (R = Et, *i*Bu, and Bn) measured in DMF under the same conditions. In DMF, the waves were found to be smaller than the analogous waves measured in CH_2Cl_2. This may indicate that **1**, **2**, and **3** react with DMF to produce other species. For **2** and **3** in CH_2Cl_2 small oxidation waves were observed. These waves are assigned to $Cu^{I/II}$ oxidation peaks of (disulfido)dicopper complexes. For **1** in CH_2Cl_2 such an oxidation wave was not observed in the same region. This may indicate that the (disulfido)dicopper(I) complex prepared by the two-electron reduction of **1** is very unstable and is subsequently decomposed. A lower energy shift of the redox wave was observed in (disulfido)Ru complexes.[49,50] These findings indicate that the disulfide ligand has a strong π-donor property.[50] Similarly, the reduction waves of **1**, **2**, and **3** were observed at –993 to –928 mV, which are in a lower potential region than the $Cu^{I/II}$ reduction waves of bis(μ-hydroxido)dicopper(II) complexes with R_3TACH $[Cu_2(OH)_2(R_3TACH)_2]^{2+}$ (R = Et, *i*Bu, and Bn) (Table 4).[51] In the reduction waves of the (disulfido)dicopper complexes in DMF and CH_2Cl_2, the reduction peaks of **1**, **2**, and **3** increase as the dihedral angles between the CuS_2 planes increase {*i*Bu (154.74°) < Et [166.12° (average)] < Bn (180°)}. These relationships may indicate that the reduction potential depends on the dihedral angle between the two CuS_2 planes.

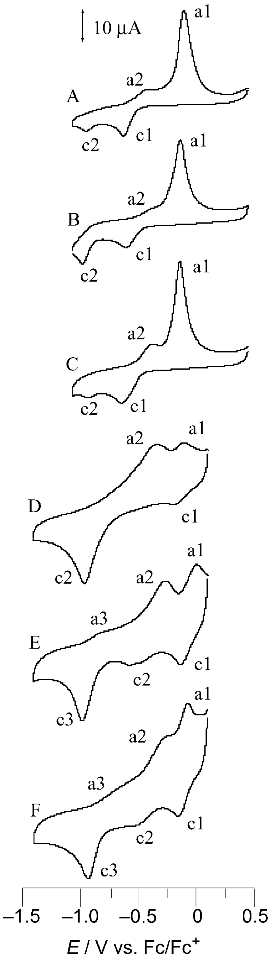

Figure 7. Cyclic voltammograms of **1** (A), **2** (B), and **3** (C) in DMF and **1** (D), **2** (E), and **3** (F) in CH_2Cl_2: 0.1 M TBAP as electrolyte; scan rate 0.1 $V s^{-1}$.

Table 4. Electrochemical data for (disulfido)dicopper complexes **1**, **2**, **3**, and bis(μ-OH)dicopper complexes with R_3TACH.[a]

Compound	DMF		CH_2Cl_2	
	E_{pa} [mV]	E_{pc} [mV]	E_{pa} [mV]	E_{pc} [mV]
1	109 (a1)	–626 (c1)	–121 (a1)	–210 (c1)
	–436 (a2)	–946 (c2)	–355 (a2)	–974 (c2)
2	–141 (a1)	–606 (c1)	–14 (a1)	–152 (c1)
	–392 (a2)	–976 (c2)	–279 (a2)	–591 (c2)
			–836 (a3)	–993 (c3)
3	–144 (a1)	–643 (c1)	–88 (a1)	–169 (c1)
	–376 (a2)	–928 (c2)	–235 (a2)	–554 (c2)
			–736 (a3)	–948 (c3)
$[Cu_2(OH)_2(Et_3TACH)_2]^{2+}$	–343	–455		
	–89			
	189			
$[Cu_2(OH)_2(iBu_3TACH)_2]^{2+}$	–281	–448		
	–41			
	129			
$[Cu_2(OH)_2(Bn_3TACH)_2]^{2+}$	–363	–465		
	–73			
	153			

[a] All potentials are reported vs. $[Fe(C_5H_5)_2]/[Fe(C_5H_5)_2]^+$ in DMF and CH_2Cl_2 at room temperature. The concentration of the supporting electrolyte TBAP was 0.1 M. The concentration of the complex was 0.5 mM. Scan rate v = 0.1 $V s^{-1}$.

Reactivity

It has previously been reported that (disulfido)dicopper(II) complexes with tris(2-pyridylmethyl)amine and bis(2-pyridylethyl)amine derivatives react with O_2, CO, PPh_3, and xylyl isocyanide,[17,48] and that the (disulfido)dicopper complex with the anilido–imine derivative reacts with PPh_3 to give $S{=}PPh_3$ and a phosphane adduct.[18] It is especially intriguing that, in an investigation reported by Tolman and co-workers, $[Cu_2(S_2)(Me_4pda)_2(CF_3SO_3)_2]$ acts as a two-electron oxidizing agent, analogous to the bis(μ-oxido)/(peroxido)dicopper system, and that substrate oxidation is accompanied by sulfur insertion in the reaction with 2,4-di-*tert*-butylphenol and 2,4-di-*tert*-butylphenolate.[21] All of the complexes **1**, **2**, and **3** demonstrate reactivity with PPh_3 to give $S{=}PPh_3$ in yields of 65 ± 3.5, 76 ± 1, and 50 ± 2%, respectively. On the other hand, Cu^I–PPh_3 adducts, $[Cu(PPh_3)(R_3TACH)]^+$, are not detected as decomposition products. Compounds **1**, **2**, and **3** are unreactive with CO, xylyl isocyanide, and benzyl bromide. Although we cannot discuss the reactivities of **1**, **2**, and **3** in detail because of their lower reactivities for substrates, the disulfur moieties of **1**, **2**, and **3** may be electrophilic judging from the results of these measurements.[17] The S–S bond lengths for **1a**, **1b**, **2**, and **3** described here are 2.101(3), 2.116(2), 2.093(6), and 2.1213(18) Å, respectively, and are almost the same as that for the (disulfido)dicopper complex with Me_2NPY2 [2.117(2) Å].[17] From the viewpoint of the S–S bond length, **1**, **2**, and **3** were expected to exhibit reactivities as high as that of $[Cu_2(S_2)(Me_2NPY2)_2][B(C_6F_5)_4]_2$. The reactivities of **1**, **2**, and **3** with PPh_3, however, were lower in comparison with the previous reports.[17] The lower reactivities of **1**, **2**, and **3** may be due to the sterically larger *N*-alkyl substituent groups on the nitrogen atoms in R_3TACH.

An interesting observation of this study is that the yields of $S{=}PPh_3$ increase as the dihedral angles of two CuS_2 planes for **1**, **2**, and **3** decrease. Although it was thought that the structures of **1**, **2**, and **3** are essentially identical in solution judging from the results of UV/Vis and resonance Raman experiments, the $Cu_2(S_2)$ plane is able to bend as shown in the crystal structures of **1b** and **2**. Thus, the bent structures may affect the reactivity with PPh_3. The relationship between the dihedral angles and the yields of products may give useful information about structure-reactivity relationships for not only (disulfido)dicopper complexes but also copper–oxygen complexes such as (μ-η^2:η^2-peroxido)- and bis(μ-oxido)dicopper complexes.

Conclusions

We have synthesized three novel (μ-η^2:η^2-disulfido)dicopper(II) complexes with *N*-alkylated *cis,cis*-1,3,5-triaminocyclohexane derivatives, **1**, **2**, and **3**. All (disulfido)dicopper complexes were characterized by spectroscopic and X-ray crystal structural analyses. From the results of crystal structural analyses and resonance Raman experiments it was indicated that the $Cu^{II}d_{xy} \rightarrow S_2^{2-}\sigma^*$ back-bonding in **1**, **2**, and **3** may be weaker than the analogous back-bonding of (μ-η^2:η^2-disulfido)dicopper complexes with diketiminate, anilido–imine derivatives, or Me_3tacn. In cyclic voltammetry experiments, **1**, **2**, and **3** gave irreversible waves. Reduction waves of **1**, **2**, and **3** shifted to a lower potential region than those of bis(μ-hydroxido)dicopper(II) complexes, indicating that strong π-donation occurs from the disulfido ligands to the Cu^{II} ion. Compounds **1**, **2**, and **3** react with PPh_3 to give $S{=}PPh_3$ in yields of 65 ± 3.5, 76 ± 1, and 50 ± 2%, respectively. The yields of $S{=}PPh_3$ depend upon the dihedral angles of the $Cu_2(S_2)$ core; the yields increase as the dihedral angle decreases. Thus, we propose that the dihedral angle of the $Cu_2(S_2)$ core influences the reactivity of the complex. This may be explained as follows: The decrease in the dihedral angle augments the π-orbital character of the S atoms and increases the reactivity of the σ-orbital.

Experimental Section

General: All reactions and manipulations of air-sensitive compounds were performed under dry Ar by using conventional Schlenk techniques or a glove box. Solvents were dried by standard methods and freshly distilled under Ar before use (e.g. diethyl ether, toluene, and THF were purified by reflux over sodium/benzophenone, and dichloromethane was refluxed over CaH_2). Electronic absorption spectra (UV/Vis spectra) were recorded with a JASCO V-570 spectrophotometer. IR spectra of the solid compounds were measured with a JASCO FT/IR-410 spectrophotometer by using the KBr disk method. X-band ESR spectra were obtained with a JEOL RE-1X spectrometer at 77 K. ^1H NMR spectral measurements were performed with a Bruker 600 MHz NMR spectrometer in $[D_6]DMSO$ by using TMS as an internal standard. Elemental analyses were performed with a Perkin–Elmer Japan 2440II CHNO/S and corrected by using acetoanilide. Electrochemical measurements were performed in a glove box by using a Bioanalytical Systems (BAS) ALS/CH Instruments Electrochemical Analyzer Model 600A, with a three-electrode system consisting of a glassy-carbon working electrode, a Pt-wire counter electrode, and an Ag/Ag^+ reference electrode. All measurements were carried out at room temperature with a sweep rate of 100 mV s^{-1} under Ar in degassed distilled DMF and CH_2Cl_2 by using nBu_4NClO_4 (TBAP) as the supporting electrolyte. The electrochemical potentials were corrected by the measurement of the ferrocene/ferrocenium $\{[Fe(C_5H_5)_2]/[Fe(C_5H_5)_2]^+\}$ couple ($E_{1/2}$ = 64 mV, ΔE = 81 mV). Electrospray ionization time of flight mass spectra (ESI-TOF/MS) were measured with a Micromass LCT spectrometer. The ligands *N,N′,N′′*-triethyl-*cis,cis*-1,3,5-triaminocyclohexane (Et_3TACH), *N,N′,N′′*-triisobutyl-*cis,cis*-1,3,5-triaminocyclohexane (*i*Bu_3TACH), and *N,N′,N′′*-tribenzyl-*cis,cis*-1,3,5-triaminocyclohexane (Bn_3TACH), and copper(I) complexes $[Cu(MeCN)(Et_3TACH)][CF_3SO_3]$, $[Cu(MeCN)(iBu_3TACH)][SbF_6]$, and $[Cu(MeCN)(Bn_3TACH)][SbF_6]$, and bis(μ-hydroxido)dicopper(II) complexes $[Cu_2(OH)_2(Et_3TACH)](CF_3SO_3)_2$, $[Cu_2(OH)_2(iBu_3TACH)](CF_3SO_3)_2$, and $[Cu_2(OH)_2(Bn_3TACH)][ClO_4]_2$ were synthesized according to previously reported methods.[31,32]

$[Cu_2(S_2)(Et_3TACH)_2](CF_3SO_3)_2$ (1): $[Cu(MeCN)(Et_3TACH)]CF_3SO_3$ (26.5 mg, 5.67×10^{-2} mmol) in CH_2Cl_2 (4 mL) was added to elemental sulfur (29.0 mg, 1.13×10^{-1} mmol). The reaction mixture was stirred for 3 h until a brown precipitate formed. The precipitate was collected and recrystallized from toluene/CH_2Cl_2 to give reddish brown crystals as **1**·$1.5CH_2Cl_2$ (16.6 mg, yield 63.9%). $C_{27.5}H_{57}Cl_3Cu_2F_6N_6O_6S_4$ (916.09): calcd. C 31.65, H 5.51, N 8.05; found C 31.74, H 5.54, N 8.20. IR (KBr): $\tilde{\nu}$ = 3220 (N–H), 2973 (aliphatic C–H), 1253 (C–F), 1155 (as, $-SO_3$), 1030 (sy, $-SO_3$) cm^{-1}. ^1H NMR ($[D_6]DMSO$, 600 MHz): δ = 4.32 (br., 2 H), 4.20 (br., 2 H), 3.79 (br., 2 H), 3.39–3.00 (br., 12 H), 2.81 (br., 4 H), 2.67 (br., 2 H), 2.21 (d, 2 H), 2.06 (br., 2 H), 1.91 (br., 2 H), 1.70–1.55 (br., 4 H), 1.42 (d, 2 H), 1.20–1.05 (br., 18 H) ppm. ESR (CH_2Cl_2, at 77 K): silent. ESI-TOF/MS: *m/z* = 765.2 $[M^+ - CF_3SO_3]$. UV/Vis reflectance: λ_{max} = 263, 348, 388, 716 nm. UV/Vis absorption (CH_2Cl_2): λ_{max} (ε_{max}) = 278 (10600 M^{-1} cm^{-1}), 359 (21100), 408 (sh, 9800), 470 (sh, 6700), 669 (750) nm.

$[Cu_2(S_2)(iBu_3TACH)_2](SbF_6)_2$ (2): Compound **2** (22.9 mg, yield 74.3%) was prepared according to the same method as **1** by using

[Cu(MeCN)(*i*Bu$_3$TACH)][SbF$_6$] (31.2 mg, 4.90×10^{-2} mmol) in place of [Cu(MeCN)(Et$_3$TACH)]CF$_3$SO$_3$, which was recrystallized from toluene/CH$_2$Cl$_2$ to give reddish brown crystals. $C_{36}H_{78}Cu_2F_{12}N_6S_2Sb_2$ (1257.77): calcd. C 34.38, H 6.25, N 6.68; found C 34.29, H 6.28, N 6.53. IR (KBr): $\tilde{\nu}$ = 3294 (N–H), 2963 (aliphatic C–H), 659 (SbF$_6^-$) cm^{-1}. ^{1}H NMR ([D$_6$]DMSO, 600 MHz): δ = 4.09 (d, 2 H), 3.74 (br., 2 H), 3.55 (d, 2 H), 3.09 (s, 2 H), 3.03 (s, 2 H), 2.96 (s, 2 H), 2.83–2.66 (m, 12 H), 2.30–2.18 (m, 6 H), 2.02–1.83 (m, 6 H), 1.84 (d, 2 H), 1.63 (d, 2 H), 1.43 (d, 2 H), 0.94–0.88 (m, 36 H) ppm. ESR (CH$_2$Cl$_2$, at 77 K): silent. ESI-TOF/MS: *m*/*z* = 1021.3 [M$^+$ – SbF$_6$]. UV/Vis reflectance: λ_{max} = 256, 360, 413, 480, 570 nm. UV/Vis absorption (CH$_2$Cl$_2$): λ_{max} (ε_{max}) = 281 (6500 M^{-1}cm^{-1}), 363 (20400), 413 (sh, 11300), 478 (sh, 7800), 671 (450) nm.

[Cu$_2$(S$_2$)(Bn$_3$TACH)$_2$](SbF$_6$)$_2$ (3): Compound **3** (21.2 mg, yield 55.1%) was prepared according to the same method as **1** by using [Cu(MeCN)(Bn$_3$TACH)][SbF$_6$] (38.9 mg, 5.26×10^{-2} mmol) in place of [Cu(MeCN)(Et$_3$TACH)][SbF$_6$], which was recrystallized from toluene/CH$_2$Cl$_2$ to give reddish brown crystals as **3**·0.5CH$_2$Cl$_2$. $C_{54.5}H_{67}ClCu_2F_{12}N_6S_2Sb_2$ (1504.34): calcd. C 43.51 H 4.49 N 5.59; found C 43.50 H 4.44 N 5.51. IR (KBr): $\tilde{\nu}$ = 3268 (N–H) , 3034 (aromatic C–H), 2933 (aliphatic C–H), 661 (SbF$_6$) cm^{-1}. ^{1}H NMR ([D$_6$]acetone, 600 MHz): δ = 7.60–7.32 (m, 30 H), 4.95 (br., 2 H), 4.53 (br., 2 H), 4.37–4.17 (m, 12 H), 4.05–3.94 (m, 2 H), 3.01 (br., 1 H), 2.88 (d, 2 H), 2.74 (br., 2 H), 2.61 (br., 2 H), 2.38 (br., 1 H), 2.26 (br., 2 H), 1.92 (br., 1 H), 1.83 (m, 1 H), 1.70 (br., 1 H), 1.54 (br., 1 H), 1.42–1.34 (m, 4 H) ppm. ESR (CH$_2$Cl$_2$, at 77 K): silent. ESI-TOF/MS: *m*/*z* = 1225.2 [M$^+$ – SbF$_6$]. UV/Vis reflectance: λ_{max} = 298, 356, 402, 450, 664 nm. UV/Vis absorption (CH$_2$Cl$_2$): λ_{max} (ε_{max}) = 295 (4700 M^{-1}cm^{-1}), 361 (17200), 402 (sh, 11000), 458 (sh, 7000), 666 (380) nm. The crystals for X-ray crystal structural analysis were recrystallized from Et$_2$O/CH$_2$Cl$_2$.

Resonance Raman Spectral Measurements: Raman scattering was excited at 457.9 nm with an Ar laser (Spectra Physics, Model 2060) and detected by using a CCD detector (Princeton Instruments, PI-CCD) attached to a single polychromator (Ritsu Oyo Kogaku, DG-1000). The slit width was set to 200 µm. The laser power used was 30 mW at the sample point. All measurements were carried out with a spinning cell (3000 rpm) at room temperature. Raman shifts were calibrated with toluene and CH$_2$Cl$_2$, and the accuracy of the peak positions of the Raman bands was ±1 cm^{-1}.

X-Ray Crystallography: Single crystals of **1**, **2**, and **3** suitable for X-ray diffraction analyses were obtained from their CH$_2$Cl$_2$/toluene or Et$_2$O solutions upon standing for a few days under Ar. Each crystal was mounted on a glass fiber, and the diffraction data were collected by using a Rigaku/MSC Mercury CCD with graphite-monochromated Mo-K_α radiation at –100 °C. Crystal data and experimental details are listed in Table 5. All three structures were solved by direct methods (SIR 92 and SHELEXS 97) and Fourier techniques. All non-hydrogen atoms were refined anisotropically. Hydrogen atoms were refined by using the riding model. A Sheldrick weighting scheme was applied. Plots of $\Sigma w(|F_o| - |F_c|)^2$ vs. $|F_o|$, reflection order in data collection, sin θ/λ, and various classes of indices showed no unusual trends. Neutral atomic scattering factors were taken from Cromer and Waber.[52] Anomalous dispersion effects were included in F_c,[53] the values for $\Delta f'$ and $\Delta f''$ were those of Creagh and McAuley.[54] The values for the mass attenuation coefficients are those of Creagh and Hubbell.[55] All calculations were performed by using the crystallographic software package CrystalStructure.[56,57] The absolute structure of **2** was deduced on the basis of the Flack parameter, 0.03(4), refined by using 2577 Friedel pairs. CCDC-671294 (**1**), -671295 (**2**), and -671296 (**3**) contain the supplementary crystallographic data for this paper. These data can be obtained free of charge from The Cambridge Crystallographic Data Centre via www.ccdc.cam.ac.uk/data_request/cif.

GC/MS Analysis of Reaction Products of 1 with PPh$_3$: A solution of PPh$_3$ (25 µL, 8 mM) in CH$_2$Cl$_2$ was added to a solution of **1** (2 mL, 0.05 mM) in CH$_2$Cl$_2$ under Ar at room temperature. The addition of *n*-hexane (2 mL) to the reaction solution produced precipitates of the Cu complexes. After filtration, the reaction products were monitored by GC/MS.

GC/MS Analysis of Reaction Products of 2 and 3 with PPh$_3$: Solutions of PPh$_3$ (50 µL, 8 mM) in CH$_2$Cl$_2$ were added to solutions of **2** and **3** (2 mL, 0.1 mM) in CH$_2$Cl$_2$ under Ar at room temperature. The addition of *n*-hexane (2 mL) to the reaction solutions produced precipitates of the Cu complexes. After filtration, the reaction products were monitored by GC/MS.

Table 5. Crystal data and experimental details for **1**, **2**, and **3**.

Compound	**1**	**2**	**3**
Empirical formula[a]	$C_{26}H_{54}Cu_2F_6N_6O_6S_4$	$C_{36}H_{78}Cu_2F_{12}N_6S_2Sb_2$	$C_{62}H_{86}Cu_2F_{12}N_6O_2S_2Sb_2$
M_r [g mol^{-1}]	909.02	1247.67	1589.94
Crystal system	triclinic	orthorhombic	monoclinic
Space group	$P\bar{1}$ (#2)	$P2_12_12$ (#18)	$P2/c$ (#13)
a [Å]	12.849(11)	13.380(16)	12.744(19)
b [Å]	17.894(4)	13.426(16)	10.467(15)
c [Å]	18.597(2)	14.37(4)	25.53(7)
α [°]	69.27(11)		
β [°]	75.04(12)		93.053(14)
γ [°]	86.71(13)		
V [Å^3]	3861(3)	2582(9)	3401(12)
Z	4	2	2
μ(Mo-K_α) [cm^{-1}]	13.922	20.012	15.407
Reflections collected	30380	19123	25506
Independent reflections (R_{int})	16938 (0.035)	5893 (0.054)	7623 (0.028)
Observed reflections [$I > 3\sigma(I)$]	11004	4153	5636
R_1[b]	0.0678	0.0721	0.0480
wR_2[b]	0.1641	0.1587	0.1242

[a] The formulae of all crystal structures are different from the formulae in the CIF files because of disordered atoms. [b] $R_1 = \Sigma||F_o| - |F_c||/\Sigma|F_o|$, $wR_2 = \{\Sigma[w(F_o^2 - F_c^2)^2]/\Sigma[w(F_o^2)^2]\}^{1/2}$.

GC/MS Conditions: Column DB-5 ms; column length 30.0 m; column temperature 100 °C (heating to 200 °C at a rate of 20 °C min^{-1} with an interval of 5 min); injection temperature 250 °C; 100 kPa. 1-chloronaphthalene was used as an internal standard.

S=PPh$_3$: t_R = 60.9 min; m/z = 294 [M$^+$].

Supporting Information (see footnote on the first page of this article): Figure S1: The cyclic voltammograms of $[Cu_2(OH)_2(R_3TACH)_2]X_2$ (R, X) = (Et, CF_3SO_3), (*i*Bu, CF_3SO_3), and (Bn, ClO_4). Figure S2: GC/MS data for products obtained from the treatment of **1**, **2**, and **3** with PPh_3 in CH_2Cl_2.

Acknowledgments

We gratefully acknowledge the support of this work from a Grant-in-Aid for Scientific Research from the Ministry of Education, Science, Sports and Culture, Kyoto-Advanced Nanotechnology Network, and in part by a grant from the NITECH 21st Century COE Program.

---

[1] B. C. Berks, S. J. Ferguson, J. W. B. Moir, D. J. Richardson, *Biochim. Biophys. Acta* **1995**, *1232*, 97–173.

[2] K. Brown, M. Prudêncio, A. S. Pereira, S. Besson, J. J. Moura, I. Moura, M. Tegoni, C. Cambillau, *Nat. Struct. Biol.* **2000**, *7*, 191–195.

[3] W. G. Zumft, *Microbiol. Mol. Biol. Rev.* **1997**, *61*, 533–616.

[4] T. Rasmussen, B. C. Berks, J. Sanders-Loehr, D. M. Dooley, W. G. Zumft, A. J. Thomson, *Biochemistry* **2000**, *39*, 12753–12756.

[5] K. Brown, K. Djinovic-Carugo, T. Haltia, I. Cabrito, M. Saraste, J. J. Moura, I. Moura, M. Tegoni, C. Cambillau, *J. Biol. Chem.* **2000**, *275*, 41133–41136.

[6] M. L. Alvarez, J. Ai, W. G. Zumft, J. Sanders-Loehr, D. M. Dooley, *J. Am. Chem. Soc.* **2001**, *123*, 576–587.

[7] P. Chen, S. I. Gorelsky, S. Ghosh, E. I. Solomon, *Angew. Chem. Int. Ed.* **2004**, *43*, 4132–4140.

[8] V. S. Oganesyan, T. Rasmussen, S. Fairhurst, A. J. Thomson, *Dalton Trans.* **2004**, 996–1002.

[9] W. B. Tolman, *J. Biol. Inorg. Chem.* **2006**, *11*, 261–271.

[10] E. I. Solomon, R. Sarangi, J. S. Woertink, A. J. Augustine, J. Yoon, S. Ghosh, *Acc. Chem. Res.* **2007**, *40*, 581–591.

[11] J. T. York, I. Bar-Nahum, W. B. Tolman, *Inorg. Chim. Acta* **2008**, *361*, 885–893.

[12] K. Fujisawa, Y. Moro-oka, N. Kitajima, *J. Chem. Soc., Chem. Commun.* **1994**, 623–624.

[13] M. E. Helton, P. Chen, P. P. Paul, Z. Tyeklár, R. D. Sommer, L. N. Zakharov, A. L. Rheingold, E. I. Solomon, K. D. Karlin, *J. Am. Chem. Soc.* **2003**, *125*, 1160–1161.

[14] E. C. Brown, N. W. Aboelella, A. M. Reynolds, G. Aullón, S. Alvarez, W. B. Tolman, *Inorg. Chem.* **2004**, *43*, 3335–3337.

[15] E. C. Brown, J. T. York, W. E. Antholine, E. Ruiz, S. Alvarez, W. B. Tolman, *J. Am. Chem. Soc.* **2005**, *127*, 13752–13753.

[16] J. T. York, E. C. Brown, W. B. Tolman, *Angew. Chem. Int. Ed.* **2005**, *44*, 7745–7748.

[17] M. E. Helton, D. Maiti, L. N. Zakharov, A. L. Rheingold, J. A. Porco Jr, K. D. Karlin, *Angew. Chem. Int. Ed.* **2006**, *45*, 1138–1141.

[18] E. C. Brown, I. Bar-Nahum, J. T. York, N. W. Aboelella, W. B. Tolman, *Inorg. Chem.* **2007**, *46*, 486–496.

[19] J. T. York, I. Bar-Nahum, W. B. Tolman, *Inorg. Chem.* **2007**, *46*, 8105–8107.

[20] M. Inosako, C. Shimokawa, H. Sugimoto, N. Kihara, T. Takata, S. Itoh, *Chem. Lett.* **2007**, *36*, 1306–1307.

[21] I. Bar-Nahum, J. T. York, V. G. Young Jr, W. B. Tolman, *Angew. Chem. Int. Ed.* **2008**, *47*, 533–536.

[22] Z. Tyeklár, K. D. Karlin, *Acc. Chem. Res.* **1989**, *22*, 241–248.

[23] N. Kitajima, Y. Moro-oka, *Chem. Rev.* **1994**, *94*, 737–757.

[24] S. Schindler, *Eur. J. Inorg. Chem.* **2000**, 2311–2326.

[25] A. G. Blackman, W. B. Tolman, *Struct. Bonding (Berlin)* **2000**, *97*, 179–211.

[26] L. M. Mirica, X. Ottenwaelder, T. D. P. Stack, *Chem. Rev.* **2004**, *104*, 1013–1045.

[27] E. A. Lewis, W. B. Tolman, *Chem. Rev.* **2004**, *104*, 1047–1076.

[28] P. Gamez, I. Koval, J. Reedijk, *Dalton Trans.* **2004**, 4079–4088.

[29] P. Chen, K. Fujisawa, M. E. Helton, K. D. Karlin, E. I. Solomon, *J. Am. Chem. Soc.* **2003**, *125*, 6394–6408.

[30] R. Sarangi, J. T. York, M. E. Helton, K. Fujisawa, K. D. Karlin, W. B. Tolman, K. O. Hodgson, B. Hedman, E. I. Solomon, *J. Am. Chem. Soc.* **2008**, *130*, 676–686.

[31] H. Arii, Y. Saito, S. Nagatomo, T. Kitagawa, Y. Funahashi, K. Jitsukawa, H. Masuda, *Chem. Lett.* **2003**, 156–157.

[32] Y. Kajita, H. Arii, T. Saito, Y. Saito, S. Nagatomo, T. Kitagawa, Y. Funahashi, T. Ozawa, H. Masuda, *Inorg. Chem.* **2007**, *46*, 3322–3335.

[33] V. H. Crawford, H. W. Richardson, J. R. Wasson, D. J. Hodgson, W. E. Hatfield, *Inorg. Chem.* **1976**, *15*, 2107–2110.

[34] M. F. Charlot, S. Jeannin, O. Kahn, J. Lucrece-Abaul, *Inorg. Chem.* **1979**, *18*, 1675–1681.

[35] M. F. Charlot, S. Jeannin, Y. Jeannin, O. Kahn, *Inorg. Chem.* **1980**, *19*, 1410–1411.

[36] P. Chaudhuri, D. Ventur, K. Wieghardt, E.-M. Peters, K. Peters, A. Simon, *Angew. Chem. Int. Ed. Engl.* **1985**, *24*, 57–59.

[37] L. J. Farrugia, P. A. Lovatt, R. D. Peacock, *Inorg. Chim. Acta* **1996**, *246*, 343–348.

[38] L. J. Farrugia, P. A. Lovatt, R. D. Peacock, *J. Chem. Soc., Dalton Trans.* **1997**, 911–912.

[39] B. Graham, M. T. W. Hearn, P. C. Junk, C. M. Kepert, F. E. Mabbs, B. Moubaraki, K. S. Murray, L. Spiccia, *Inorg. Chem.* **2001**, *40*, 1536–1543.

[40] B. Graham, L. Spiccia, G. D. Fallon, M. T. W. Hearn, F. E. Mabbs, B. Moubaraki, K. S. Murray, *J. Chem. Soc., Dalton Trans.* **2002**, 1226–1232.

[41] A. J. Evans, S. E. Watkins, D. C. Craig, S. B. Colbran, *J. Chem. Soc., Dalton Trans.* **2002**, 983–994.

[42] D. Rojas, A. M. Garcia, A. Vega, Y. Moreno, D. Venegas-Yazigi, M. T. Garland, J. Manzur, *Inorg. Chem.* **2004**, *43*, 6324–6330.

[43] C.-C. Chou, C.-C. Su, H.-L. Tsai, K.-H. Lii, *Inorg. Chem.* **2005**, *44*, 628–632.

[44] M. J. Belousoff, M. B. Duriska, B. Graham, S. R. Batten, B. Moubaraki, K. S. Murray, L. Spiccia, *Inorg. Chem.* **2006**, *45*, 3746–3755.

[45] A. W. Addison, T. N. Rao, J. Reedijk, J. van Rijn, G. C. Vershoor, *J. Chem. Soc., Dalton Trans.* **1984**, 1349–1356.

[46] K. D. Karlin, J. C. Hayes, J. P. Hutchinson, J. Zubieta, *Inorg. Chem.* **1982**, *21*, 4106–4108.

[47] K. Nakamoto, *Infrared and Raman Spectra of Inorganic and Coordination Compounds Part B*, 5th ed., John Wiley & Sons, Inc., New York, **1997**, pp. 199–256.

[48] D. Maiti, J. S. Woertink, M. A. Vance, A. E. Milligan, A. A. Narducci Sarjeant, E. I. Solomon, K. D. Karlin, *J. Am. Chem. Soc.* **2007**, *129*, 8882–8892.

[49] J. Amarasekera, T. B. Rauchfuss, R. S. Wilson, *Inorg. Chem.* **1987**, *26*, 3328–3332.

[50] K. Matsumoto, T. Matsumoto, M. Kawano, H. Ohnuki, Y. Shichi, T. Nishida, T. Sato, *J. Am. Chem. Soc.* **1996**, *118*, 3597–3609.

[51] The reduction peaks of $[Cu_2(OH)_2(R_3TACH)_2]^{2+}$ (R = Et, *i*Bu, and Bn) were observed at –455, –448, and –465 mV vs. $[Fe(C_5H_5)_2]/[Fe(C_5H_5)_2]^+$, and the oxidation peaks were observed at –343, –89, and 189 mV for $[Cu_2(OH)_2(Et_3TACH)]^{2+}$, –281, –41, and 129 mV for $[Cu_2(OH)_2(i\text{Bu}_3TACH)_2]^{2+}$, –363, –73, and 153 mV for $[Cu_2(OH)_2(Bn_3TACH)_2]^{2+}$, respectively. Among these oxidation peaks, two additional positive peaks were observed that may represent oxidation waves of other complexes formed from the reaction of bis(μ-OH)dicopper complexes with the DMF electrolyte.

[52] D. T. Cromer, J. T. Waber, *International Tables for X-ray Crystallography*, Kynoch Press, Birmingham, UK, **1974**, vol. 4.
[53] J. A. Ibers, W. C. Hamilton, *Acta Crystallogr.* **1964**, *17*, 781.
[54] D. C. Creagh, W. J. McAuley, *International Tables for X-ray Crystallography*, Kluwer, Boston, **1992**, vol. C, Table 4.2.6.8, pp. 219–222.
[55] D. C. Creagh, J. H. Hubbell, *International Tables for Crystallography*, Kluwer, Boston, **1992**, vol. C, Table 4.2.4.3, pp. 200–206.
[56] *CrystalStructure 3.7.0 – Crystal Structure Analysis Package*, Rigaku and Rigaku/MSC, The Woodlands, TX, **2000–2005**.
[57] D. J. Watkin, C. K. C. Prout, J. R. Carruthers, P. W. Betteridge, *CRYSTALS Issue 10*, Chemical Crystallography Laboratory, Oxford, **1996**.

Received: December 21, 2007